In: Neurocomputing: Learning, Architectures and ModelingISBN 978-1-61324-699-3
Editor: Elizabeth T. Mueller

Chapter 4

COMPARISON OF EEG MONTAGES FOR DIAGNOSIS OF ALZHEIMER'S DISEASE USING SPECTRAL FEATURES AND SUPPORT VECTOR MACHINES

Trambaiolli, L.R. .[1a]; Lorena, A.C.[2a]; Fraga, F.J.[3b] ; Anghinah R.[4c]

[a] Mathematics, Computing and Cognition Center (CMCC), Universidade Federal do ABC (UFABC), Rua Santa Adélia, 166 - CEP: 09.210-170 - Santo André - SP - Brazil

[b] Engineering, Modeling and Applied Social Sciences Center (CECS), Universidade Federal do ABC (UFABC), Rua Santa Adélia, 166 - CEP: 09.210-170 - Santo André - SP - Brazil

[c] Reference Center of Behavioral Disturbances and Dementia (CEREDIC) and Neurology Department of Medicine School of University of São Paulo (USP)
Rua Arruda Alvim, 206 - CEP: 05.410-020 - São Paulo - SP – Brasil

[1] Email: lucasrtb@yahoo.com.br
[2] Email: aclorena@gmail.com
[3] Emal: franciscojfraga@gmail.com
[4] Email: anghinah@usp.br

ABSTRACT

In this chapter we calculated electroencephalogram (EEG) spectral peaks with different electrode montages and studied their predictive ability when used as features in the automatic differentiation of Alzheimer's disease (AD) patients from controls. During the evaluation process we used statistical analysis, automatic feature selection and Support Vector Machine (SVM) classification. Among the montages studied, Bipolar Homologous presented the best classification (AD vs. controls) performance, with 85.29% accuracy, 90.91% sensitivity and 75.00% specificity. We demonstrated that differences between montages are statistically significant depending on frequency bands and scalp regions considered. When working with automatic feature selection, it was possible to reduce the total set of 345 features (sum of EEG spectral peaks from all montages) to 24 using the Consistency-Based Filter (CBF) feature selection algorithm and rank search, with minor decreasing in subjects classification performance.

1. INTRODUCTION

Alzheimer's disease (AD) is considered the leading cause of dementia in Western countries [1], manifested by memory loss and impairment of at least another area of cognition (calculation, praxis, gnosis, executive functions, language, etc.). As definitive diagnosis of AD can only be established by histopathological analysis of the brain (necropsy or biopsy) [2], the challenge for the search of a biological marker to determine early and more accurate diagnosis of the disease remains open. Currently, correct diagnosis by neuropsychological tests ranges from 85% to 93% accuracy in university hospitals, but these cognitive screening batteries are not easy to apply, requiring experienced and lengthy sessions [3].

One test used as an alternative tool for the diagnosis of dementia is the electroencephalogram (EEG) [4], which is the record of different rhythms and voltages from synaptic activity between neurons [5]. The literature shows that the average EEG alpha rhythm of elderly is about 10 Hz, and a significant lower value probably indicates pathologies [6, 7, 8, 9].

A simple spectral feature used to characterize EEG rhythms is the peak of the spectrum (spectral peak), which measures the frequency where the

magnitude of the short-time spectrum – usually obtained by Fast Fourier Transform (FFT) – of the EEG signal reaches its maximum value.

It had previously shown that peaks smaller than 8.0 Hz could be considered pathological [8] and peaks higher than 10.0 Hz could be considered normal [10]. But the range between 8.0 and 10.0 Hz could be shared by both groups. It was also demonstrated that distinct electrode montages can also influence the accuracy of EEG-based AD diagnosis [11].

This chapter presents an evaluation through computer techniques, showing how different electrode montages can positively or negatively influence automatic classification of normal subjects and those with AD. We used feature selection algorithms based on the filter approach and statistical analysis as preprocessing for the Support Vector Machine (SVM) classifier.

In Section 2 we show the methodology used, while in Sections 3 and 4 we present and discuss, respectively, the experimental results. Finally, in Section 4 we presents our conclusions.

2. MATERIALS AND METHODS

2.1. Dataset

The data set used in this work comprises EEG exams of subjects with and without the disease (controls). We selected two groups of volunteers: the first (G1) is composed of 12 normal subjects (68.8 ± 6.7 years, 8 women) and the second (G2) is composed of 22 (probable) AD patients (71.5 ± 7.7, 17 women). AD diagnosis was performed according to NINCDS-ADRDA criteria [12], being classified as mild to moderate, according to DSM-III R [13]. Subjects had no history of diabetes mellitus, kidney diseases, thyroid diseases, alcoholism, liver disease, lung disease or lack of vitamin B12, factors that can disturb cognitive impairment diagnosis.

EEG records were obtained with an equipment brand EMSA, 32-channel, 12 bits A/D converter and sampling rate of 200 Hz. Placement of scalp electrodes (Fp1, Fp2, Fz, F3, F4, F7, F8, C3, C4, Pz, P3, P4, T5, T6, O1 and O2) followed the international 10-20 system (Figure 1). We used inter-connected ear lobe electrodes reference (electrodes A1 and A2), as recommended by the Brazilian Society of Clinical Neurophysiology and the American EEG Society. During examination, subjects were awake and resting with eyes closed.

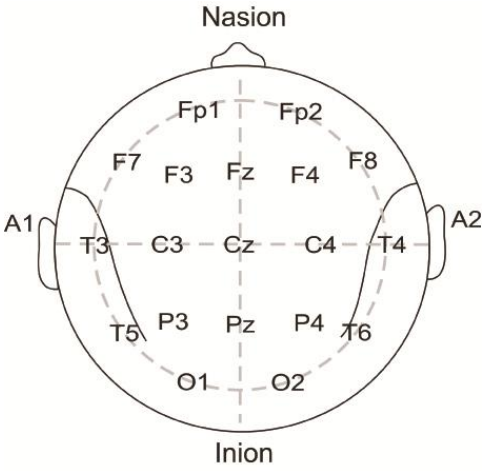

Figure 1. International 10-20 System.

2.2. Preprocessing

Aided by a skilled physician, we selected 40 epochs (all channels) with eight seconds each by visual inspection, to remove artifacts, i.e., any electrical potential from a source other than the brain, such as blinking, muscle movements or equipment-related potentials [14].

EEG signals (EEGs) were low-pass filtered with cutoff frequency at 50Hz. The digital filter used had a zero at 60Hz, thus eliminating any interference from the power grid. The frequency analysis was performed with a 512-point Fast Fourier Transform algorithm, using Hamming windows with 2.5 s duration and 0.25 s increment between successive windows (90% overlap).

We divided EEGs into the well-known delta (0.1 to 4.0 Hz), theta (4.0 to 8.0 Hz), alpha (8.0 to 12.0 Hz), beta (12.0 to 30.0 Hz) and gamma (30.0 to 100.0 Hz) bands [14].

2.3. Feature Extraction

The spectral peak feature (or peak spectrum), chosen for this work, corresponds to the frequency where the EEG spectrum amplitude reaches its

maximum value. The combinations of electrodes (montages) used in its calculation, as can be seen in Figure 2, were between:

- Peaks with bi-auricular reference (Pba): Fp1-A1, Fp2-A2, F7-A1, A2-F8, F3-A1, F4-A2, A1-C3, C4-A2, A1, T3, T4-A2, P3 -A1, P4-A2, A1-T5, T6-A2, O1-A1, O2-A2;
- Peaks with Cz reference (PCz): Fp1-Cz, Fp2-Cz, Cz-F3, F4, Cz, Cz-F7, F8, Cz, T3-Cz, T4-Cz, Cz-C3, C4, Cz, T5 -Cz, T6-Cz, Cz-P3, P4-Cz, Cz-O1, O2-Cz;
- Longitudinal bipolar peaks (Lbp): Fp1-F3, F3-C3, C3-P3, P3-O1, O1-T5, T5-T3, T3-F7, F7-Fp1, Fp2-F4, F4-C4, C4-P4, P4-O2, O2-T6, T6-T4, T4-F8, F8-Fp2;
- Bipolar cross peaks (Bcr): Fp1-Fp2, F7-F3, F3-Fz, Fz-F4, F4-F8, T3-C3, C3-Cz, Cz-C4, C4-T4, T5-P3, P3-Pz, Pz-P4, P4-T6, O1-O2;
- Bipolar counterparts peaks (Bco): F7-F8, F3-F4, T3-T4, C3-C4 P3-P4, T5-T6 O1-O2.

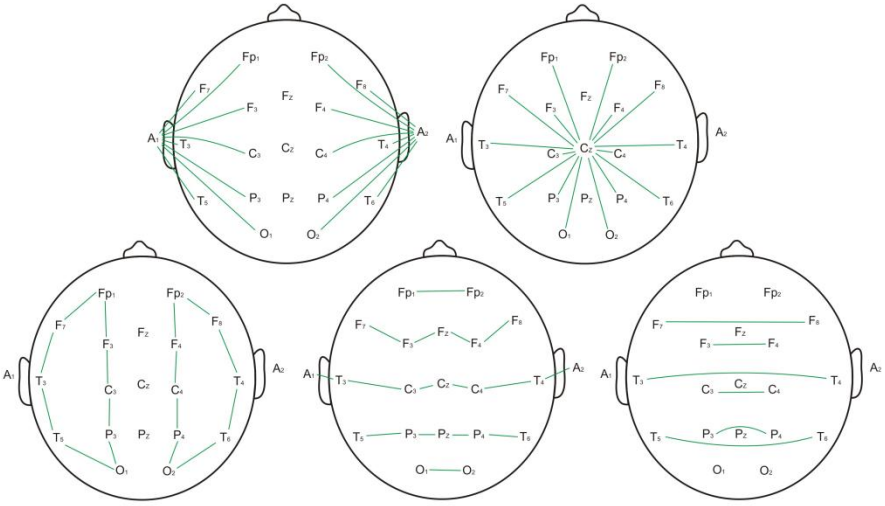

Figure 2. Maps of spectral peaks montages, where the lines correspond to subtractions used to calculate the spectral peaks. From left to right, top to botton: peaks with Biauricular Reference, peaks with Reference in Cz, Longitudinal Bipolar peaks, Transverse Bipolar peaks and Homologous Bipolar peaks.

2.4. Support Vector Machines

Support Vector Machines (SVMs) constitute a supervised Machine Learning (ML) technique based on the Statistical Learning Theory [25]. In this method, a training dataset (containing known labeled data examples) is used to draw a hyperplane with maximum margin, based on the feature coordinates, which separates the two classes (in our case, Controls and AD). Subsequently, the coordinates of this hyperplane are used to test a dataset, and the accuracy of the model [26]. When classes are not linearly separable, feature coordinates should be mapped to a higher dimension by a Kernel function. In this new space, the classes become linearly separable and the maximum margin hyperplane can then be found [26].

The Weka tool [27] with default values was used to the SVM induction. The SVM regularization coefficient was C=1.0. We used the RBF Kernel, which is proved to be more effective in previous [28]. The cache size was 250007, and the gamma value was 0.01

The EEG dataset was composed of 1360 epochs (40 epochs of 34 subjects). The analysis was based on the leave-one-subject-out (LOSO) process: 1320 epochs were used for training and 40 epochs from one subject for testing. It means that, each time, the classifier was trained with epochs from all individuals except the one going to be tested. This procedure was performed to test the SVM discriminative capacity to work with data diverse from that presented in the training period. The LOSO process was repeated for all 34 individuals (34 tests each montage).

2.5. Feature Selection

In this step we considered two filter approach algorithms. The first is CFS (Correlation-based Feature Selection), which evaluates the quality of feature subsets taking into account the criteria of relevance and non-redundancy [19]. The second approach is CBF (Consistency Based Filter), which uses the selection of subsets with few high consistency features. This allows splitting data so that most examples not contained in each partition are labeled with the majority class [20]. In both cases, selection was performed using the Weka tool [17].

The search algorithms used for feature selection were [Witten and Frank, 2005]:

- *BestFirst*, which performs greedy search in the space of feature subsets. It starts with an empty set of features and perform forward search, or starts with the complete set of features and perform backward search. A third possibility is beginning at any point in space and performing search in both directions (considering all possible additions and deletions of feature at one point). It is used with the CFS selection algorithm.
- *GreedyStepwise*, which runs forward or backward greedy search through the space of feature subsets. It can start from an arbitrary point in space, without any (or all) features, stopping when the addition/exclusion of the other features result in reduced evaluation. It can also produce an ordered list of features across space from one side to another and recording the order in which they are selected. It is used with CBF algorithm.
- *RankSearch*. It evaluates the subsets, which are then submitted to a forward selection to generate an ordered list (where the best subset of features is reported). It is used with both selection algorithms.

Feature selection tests also followed the LOSO procedure, where each group of 33 patients (1320 epochs) was submitted to the selection algorithm. At the end of the process, for each test the selected features form the new training and test sets to the SVMs.

3. RESULTS AND DISCUSSION

The leave-one-out analysis of each subject took into consideration the ratio between the number of epochs classified correctly and the total number of epochs. When this ratio was over 0.5, the subject classification was considered correct. After 34 tests, the rate of subject correct diagnosis was calculated.

Table 1 presents the classification results for each electrode montage, and also considering all electrodes (all peaks). Bco gives the best results in the classification of epochs, and also the best rates of accuracy and specificity in subjects classification. The best sensitivity rate in the classification of subjects is achieved by Pba montage.

Table 1. Classification results by epochs and by patients. The best results are in bold font and worst in italic

	Epochs			**Subjects**		
	Accuracy (%)	***Sensibility (%)***	***Specificity (%)***	***Accuracy (%)***	***Sensibility (%)***	***Specificity (%)***
Pba	70,07±36,81	85,57±23,12	*41,67±41,03*	76,47	**95,45**	*41,67*
PCz	70,22±37,70	81,36±31,15	49,79±41,33	70,59	*81,82*	50,00
Lpb	72,72±36,8	84,09±27,52	51,88±43,39	79,41	90,91	58,33
Bcr	*69,19±37,60*	*80,23±32,40*	48,96±39,32	*64,71*	*81,82*	*41,67*
Bco	**81,32±28,00**	**89,43±20,92**	**66,46±33,84**	**85,29**	90,91	**75,00**
All	75,66±34,96	85,45±28,56	57,71±39,56	73,53	86,36	50,00

Good performance of Bco montage is consistent with previous studies that suggest bipolar montages present better results than referential montages [11]. When compared to the configuration of all montages together, Bco gets about 6% and 12% advantage in the accuracy of epochs and subjects, respectively.

Statistical analysis was performed using the two-tailed Student t-test for different means and variances. Significance ($p<0.05$) was observed for a large number of features of all montages. Features related to alpha band show statistical significance for all electrodes of all montages ($p <0.01$). Spectral peaks (DA and normal) mean and standard deviation values of this band are plotted in Figure 3 for Bco montage. In the figure one can see that patients with AD (plotted in red) have lower alpha spectral peaks than normal subjects, as predicted in the literature [21, 22, 23].

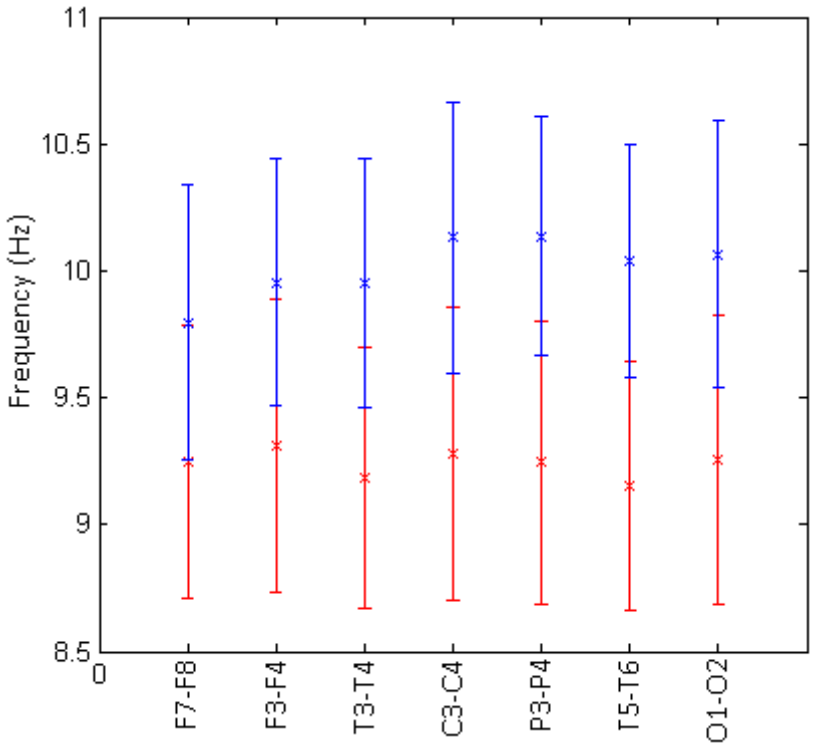

Figure 3. Spectral peaks mean and standard deviation values of alpha band (Bco montage), showing DA in red and Normal in blue.

Table 2. Classification results by epochs and by patients in selected subsets. Best results are in bold font and worst in italic

	Epochs			**Patient**		
	Accuracy (%)	***Sensibility (%)***	***Specificity (%)***	***Accuracy (%)***	***Sensibility (%)***	***Specificity (%)***
CBF Greedy	*73,90±32,92*	88,52±23,66	*47,08±31,15*	85,29	95,45	*66,67*
CBF Rank	81,03±30,57	86,25±27,97	71,46±33,99	82,35	*86,36*	75
CFS BestFirst	79,19±29,95	*85,11±28,11*	68,33±31,38	*79,47*	*86,36*	*66,67*
CFS Rank	80,51±30,11	85,34±28,98	71,67±31,38	82,35	*86,36*	75

Regarding the feature selection algorithms, the best result in the classification of patients is obtained by Greedy-CBF (CBF-G), which present a performance similar to Bco. However, considering epochs classification it is the one with less specificity.

Otherwise, Rank-CBF (CBF-R) is more balanced considering both epochs and subjects classification performance. So, in Table 3 we show only the selected features in at least 50% of LOSO tests using the CBF-R algorithm. For each feature in the table, we show its selection rate (%), i.e., the percentage of LOSO tests in which the feature was selected.

Among the selected features, it can be verified a predominance of alpha-band, followed by gamma-band electrodes. Analyzing all electrode montages, we can find six Bco features, seven Bcr features, six Lbp, nine electrodes of PCz and no electrodes of Pba montages.

One can see that with the exception of F4-C4 and Fp1-F3, all other selected features belong to the posterior half of the scalp, a result interesting and congruent with literature from other spectral features [10, 26, 27].

The presence of gamma-band features is interesting, since this rhythm is related to cognitive activity, directly affected by AD. Previous studies had already found reduced values of gamma rhythm when compared to healthy individuals [28, 29].

It is also worth to discuss the meaning of selection algorithms. The CBF algorithm suggests that 24 selected features (CBF-R test), against 345 original features with minor performance reduction is a promising result [20].

The CFS algorithm is based in the search for relevant and not redundant features. However, subsets selected by the algorithm did not achieve good predictive results [19].

4. CONCLUSION

Although more tests are needed to confirm our findings, we showed that spectral peak calculation using different montages of electrodes have influence in the classification results of normal subjects and patients with AD. We also demonstrated that alpha and gamma features are more relevant in AD classification, and feature selection techniques are promising towards the search for simple and effective EEG-based AD biomarkers. Our future goal is to generalize the results obtained increasing the number of subjects.

Table 3. Selected Features to CBF-Rank subsets

Feature	Selection rate (%)	Feature	Selection rate (%)
Bco - T3-T4-alpha	100	Bco/Bcr - O1-O2-alpha	97.06
Bco - P3-P4-alpha	100	Lbp - O1-T5-alpha	94.12
Bco - T5-T6-alpha	100	PCz - O1-Cz-alpha	94.12
Lbp - C3-P3-alpha	100	Bco - C3-C4-alpha	88.24
Bcr - P3-Pz-alpha	100	PCz - P4-Cz-alpha	85.29
Bcr - Pz-P4-alpha	100	Lbp - F4-C4-alpha	79.41
PCz - T3-Cz-alpha	100	Pba - O2-A2-alpha	79.41
PCz - P3-Cz-alpha	100	PCz/Bcr - C4-Cz-alpha	73.53
PCz - T5-Cz-alpha	100	PCz/Bcr - C4-Cz-gamma	67.65
Bco/Bcr - O1-O2-alpha	97.06	Lbp - Fp1-F3-gamma	58.82
Lbp - F4-C4-gamma	97.06	Lbp - O2-T6-alpha	58.82
PCz/Bcr - C3-Cz-alpha	97.06	PCz - P3-Cz-gamma	58.82

REFERENCES

[1] Bird, T. D. (2001). Alzheimer's disease and other primary dementias. In Braunwald, E., Fauci, A. S., Kasper, D. L., Hauser, S. L., Longo, D. L., & Jameson, J. L. (Ed.), Harrison's principles of internal medicine, (2391–2399). New York: McGraw-Hill.

[2] Terry, R. (1994). Neuropathological changes in Alzheimer disease. *Progress in brain research*, 101, 383–390.

[3] Parikh, D., Stepenosky, N., Topalis, A., Green, D., Kounios, J., Clark, C., & Polikar, R. (2005). Ensemble Based Data Fusion for Early Diagnosis of Alzheimer's Disease. In 27th Annual International Conference of the Engineering in Medicine and Biology Society, 2479–2482.

[4] Luccas, F., Braga, N., Fonseca, L., & Frochtengarten, M. (1996). Recomendações para o registro e interpretação do mapeamento topográfico do eletrencefalograma (EEG) e potenciais evocados sensoriais (PES) parte I: aspectos gerais [in portuguese]. *Brazilian Journal Epilepsy Clinical Neurophysiology*, 2, 175–182.

[5] Epstein, C. (1995). Digital EEG: choosing the right equipment for your lab. 30th Annual Course in Clinical EEG and Electrophysiology of American EEG Society, 1–11.

[6] Hughes, J. & Cayaffa, J. (1977). The EEG in patients at different ages without organic cerebral disease. *Electroencephalography and clinical neurophysiology*, 42(6), 776-784.

[7] Katz, R. & Horowitz, G. (1982). Electroencephalogram in the septuagenarian: studies in a normal geriatric population. *Journal of the American Geriatrics Society*, 30(4), 273.

[8] Arenas, A., Brenner, R., & Reynolds, C. (1986). Temporal slowing in the elderly revisited. *American Journal EEG Technology*, 26, 105–114.

[9] Niedermeyer, E. (1993). The normal EEG of the waking adult. In Niedermeyer, E. & Lopes da Silva, F. H. Electroencephalography. Philadelphia: Williams & Wilkins.

[10] Anghinah, R. (2003). Estudo da densidade espectral e da coerência do eletroencefalograma em indivíduos normais e com doença de Alzheimer provável [in portuguese]. PhD thesis. São Paulo: São Paulo University Medical School.

[11] Trambaiolli, L. R., Lorena, A. C., Fraga, F. J. & Anghinah, R. (2010). Support vector machines in the diagnosis of Alzheimer's disease. In

IEEE Proceedings of the ISSNIP Biosignals and Biorobotics Conference, 1–6.

[12] McKhann, G., Drachman, D., Folstein, M., Katzman, R., Price, D. & Stadlan, E. (1984). Clinical diagnosis of Alzheimer's disease: Report of the NINCDS-ADRDA Work Group* under the auspices of Department of Health and Human Services Task Force on Alzheimer's Disease. *Neurology*, 34(7), 939-944.

[13] Spitzer, R. & Williams, J. (1992). Structured clinical interview for DSM-III-R (SCID): User´s guide. Washington: American Psychiatric Publishing.

[14] Sanei, S. & Chambers, J. (2007). EEG signal processing. West Sussex: Wiley-Interscience.

[15] Vapnik, V. N. (1995). The nature of Statistical learning theory. New York : Springer-Verlag,.

[16] Cristianini, N. & Shawe-Taylor, J. (2000). An introduction to support Vector Machines: and other kernel-based learning methods. Cambridge: Cambridge University Press.

[17] Witten, I. A. & Frank, E. (2005). Data Mining: Practical Machine Learning Tools and Techniques. San Francisco: Elsevier.

[18] Trambaiolli, L. R., Lorena, A. C., Fraga, F. J. & Anghinah, R. (2009). Uso de aprendizado de máquina no auxílio ao diagnóstico de Alzheimer [in portuguese]. *REIC - Revista Eletrônica de Iniciação Científica*, 9(3), 1–14.

[19] Hall, M. & Holmes, G. (2003). Benchmarking attribute selection techniques for discrete class data mining. *IEEE Transactions on Knowledge and Data engineering*, 15(6), 1437-1447.

[20] Liu, H. & Setiono, R. (1996). A probabilistic approach to feature selection - a filter solution. In *Machine Learning-International Workshop Then Conference*, 319-327.

[21] Leuchter, A.F., Spar, J.E., Walter, D.O. & Weiner, H. (1987). Electroencephalographic spectra and coherence in the diagnosis of Alzheimer's-type and multi-infarct dementia. A pilot study. *Archives of General Psychiatry*, 44, 993-998.

[22] Dierks, T., Perisic, I., Frölich, L., Ihl, R. & Maurer, K. (1991). Topography of the qEEG in dementia of Alzheimer type: relation to severity of dementia. *Psychological Research*, 40, 181-194.

[23] Leuchter, A. F., Cook, I. A., Newton, T. F., Dunkin, J., Walter, D. O., Thompson, S. R., Lachenbruch, P. A. & Weiner, H. (1993). Regional differences in brain electrical activity in dementia: use of spectral

power and spectral ratio measures. *Electroencephalography and Clinical Neurophysiology*, 87, 385-393.

[24] Coben, L. A., Danziger, W. L. & Berg, L. (1983). Frequency analysis of the resting awake EEG in mild senile dementia of Alzheimer type. *Electroencephalography Clinical Neurophysiology*, 55, 372–380.

[25] Coben, L. A., Danziger, W. & Storandt, M. (1985) A longitudinal EEG study of mild senile dementia of Alzheimer type: changes at 1 year and at 2.5 years. *Electroencephalography Clinical Neurophysiology*, 61, 101–112.

[26] Locatelli, T., Cursi, M., Liberati, D., Franceschi, M., and Comi, G. (1998). EEG coherence in Alzheimer's disease. *Electroencephalography and clinical neurophysiology*, 106(3), 229-237.

[27] Akrofi, K., Baker, M., O'Boyle, M., and Schiffer, R. (2008). Clustering and Modeling of EEG Coherence Features of Alzheimer's and Mild Cognitive Impairment Patients. In *Annual International Conference of the IEEE Engineering in Medicine and Biology Society*, 1, 1092-1095.

[28] Herrmann, C.S. & Demiralp, T. (2005). Human EEG gamma oscillations in neuropsychiatric disorders. *Clinical Neurophysiology*, 116, 2719–2733.

[29] Koenig, T., Prichep, L., Dierks, T., Hubl, D., Wahlund, L.O., John, E.R. & Jelic, V. (2005). Decreased EEG synchronization in Alzheimer’s disease and mild cognitive impairment. *Neurobiology Aging*, 26, 165–171.